Dicle University
Journal of Engineering
https://dergipark.org.tr/tr/pub/dumf
duje.dicle.edu.tr

Research Article

Key Factors that Affect the Behavior of Steel Beams and Columns in Special Moment Frames

Gülen Özkula[1*]

[1] Tekirdağ Namık Kemal Üniversitesi, İnşaat Mühendisliği Bölümü, gozkula@nku.edu.tr
ORCID: https://orcid.org/0000-0002-1947-6362

ARTICLE INFO

Article history:

Received 17 October 2022
Received in revised form 5 April 2023
Accepted 18 June 2023
Available online 20 June 2023

Keywords:

Special Moment Frames, Deep columns, Column bracing, Beam bracing

Doi: 10.24012/dumf.1190792

* Corresponding author

ABSTRACT

Steel Special Moment Frames (SMFs) are favored seismic force-resisting systems due to their architectural flexibility and high ductility. While shallow columns (section depth less than 356 mm) were commonly used in these systems before the Northridge earthquake, deeper columns (section depth greater than 356 mm) have become more popular in recent years to meet code-enforced story drift requirements economically. However, limited research exists on the hinging behavior of deep columns under axial compression and cyclic drift. Since deep columns exhibit larger slenderness ratios and are more susceptible to local and global buckling, understanding their behavior is crucial. This study investigates the behavior of fifteen four-story steel SMFs using finite element program simulations, focusing on four key factors affecting frame behavior: 1) Column bracing, 2) Beam bracing, 3) Column stiffening, and 4) Strong Column Weak Beam (SCWB) ratio. The influence of axial force level and column section properties is also examined. Results demonstrate that deep columns may experience local and/or global instabilities at relatively low story drift levels. Findings suggest that SMF performance can be enhanced by bracing deep columns at the top and bottom levels of beam flanges and adding stiffeners to the columns' web. Controlling column shortening by increasing the SCWB ratio is also recommended.

Introduction

Steel special moment frames (SMFs) are widely used as seismic force-resisting systems (SFRS) in high-seismic regions due to their architectural flexibility and high ductility capacity. The unexpected non-ductile failure of seismically designed steel moment connections observed after the Northridge, California earthquake prompted extensive research into the behavior of these SMFs. Significant studies have been conducted to examine the cyclic behavior and design of beam-to-column connections, including work by the SAC Joint Venture [1]. While the cyclic behavior of beams has been extensively investigated, as plastic hinging is anticipated in an SMF, the behavior of columns has received less attention.

Various experimental studies have shown that a structural component's hysteretic behavior depends on numerous factors that significantly influence its deformation and energy dissipation characteristics. Consequently, collapse assessment methodologies for structural systems with component deterioration have been proposed by [2] and [3], based on the fundamentals outlined by [4]. Lignos and Krawinkler [5] revised the deterioration models for beams with reduced beam sections (RBS) and non-RBS members. Newell and Uang [6] evaluated nine full-scale W14 columns for use in braced frames, demonstrating that stocky columns can achieve substantial inelastic story drift capacities (0.75Py) even under strong axial stresses.

Before the Northridge earthquake, shallow columns (section depth less than 356 mm) were commonly used in these SFRSs. However, to meet code-enforced story drift criteria and achieve design economy, deeper columns have become increasingly popular in recent years. Despite their widespread use, limited research has been conducted on the behavior of these columns under axial compression and cyclic drift. Examining the behavior of deep columns is crucial, as they have higher slenderness ratios and are more susceptible to both local and global buckling. Newell and Uang's [6] numerical studies revealed that deep W27 columns subjected to high axial loads experience rapid strength degradation due to simultaneous flange and web local buckling.

Elkady and Lignos [7] later employed finite element modeling to investigate the behavior of deep beam-columns, observing both axial shortening and significant strength deterioration as a result of local buckling. Cheng et al. [8] subjected nine wide-flange cantilever members with large width-to-thickness ratios to cyclic lateral

displacement under constant axial loads for weak-axis bending. Local instabilities were identified as the cause of each member's failure mechanism, leading the authors to conclude that the section categorization procedures in the current design requirements are unsuitable for wide-flange sections bent around their weak-axis.

Fogarty and El-Tawil [9] used detailed finite element models to assess the response of deep columns, finding that many deep columns meeting the AISC high ductility criteria were unable to achieve 4% lateral drift under axial loads between $0.2P_y$ and $0.4P_y$. The web's width-to-thickness ratio has a greater impact than the flange's. Suzuki and Lignos [10] tested lighter W14 cantilever columns using various loading protocols, determining that realistic loading histories are necessary for calibrating component deterioration models. These protocols should also capture the member's ratcheting effect before failure. Wu et al. [11] emphasized the importance of selecting appropriate loading histories when analyzing the collapse of deep columns using finite element modeling.

To explore the cyclic response of these columns for use in SMFs, Ozkula et al. [12] and [13] conducted forty-eight full-scale deep column tests. This test program's data were used to: (1) calibrate analytical models; (2) build a comprehensive database on deep columns; (3) classify sections according to their buckling modes; (4) assess the suitability of AISC 341's design provisions for seismic design of new construction; and (5) evaluate ASCE 41's design provisions for seismic assessment of existing construction. Although the cross-sections of these columns met the highly ductile (λ_{hd}) condition outlined in the AISC Seismic Provisions or AISC 341 [14], the authors demonstrated that deep columns could undergo significant buckling and axial shortening for use in SMFs. Web local buckling (WLB) interacted with flange local buckling (FLB), which was not considered by AISC 341, resulting in substantial shortening. Testing shallow and stocky W14 columns [6] did not reveal significant column shortening, as WLB did not occur. Some column tests also uncovered an "unexpected" failure scenario involving both local buckling and lateral-torsional buckling (LTB). A parametric analysis of 110 beam-columns was conducted using high-fidelity ABAQUS [15] nonlinear finite element simulations to cover a wide range of slenderness ratios, axial force levels, and yield stresses, aiming to improve the database for both cyclic modeling and design recommendations.

Majority of the previous studies focused on member-level analysis of deep columns. In this study, ABAQUS CAE [15] was used to model a subassembly of deep columns to investigate the effects of column bracing, beam bracing, column stiffening, and the Strong Column Weak Beam (SCWB) ratio. The findings indicated that bracing deep columns at the top and bottom levels of the beam flanges and adding stiffeners to the web of these columns could enhance the performance of SMFs. The concept is that by increasing the SCWB ratio, column shortening can be prevented.

Arctype Building

Prior studies [13] have shown that the hysteretic response of columns is characterized by the beam-column buckling mode. The governing buckling mode, or failure mode, can be categorized into three types: (1) Symmetric Flange Local Buckling (SFB) mode, (2) Anti-symmetric Local Buckling (ALB) mode, and (3) Coupled Buckling (CB) mode. Ozkula et al. [13] proposed predicting these modes using a parameter based on the section slenderness properties within a certain limit of L/r_y. In this study, the observed column behaviors are explained using the failure mode classifications suggested by Ozkula et al. [13].

The primary motivation for the configuration of the new archetype building was the use of deep slender columns tested by Ozkula et al. [13]. As the main objective in the design of the archetype building was to validate the accuracy of the component-level test results, the first-story columns for the archetype building were selected from the columns tested by Ozkula et al. [12] and Newell and Uang [6]. This allowed for the observation of the behavior of sections that failed in SFB, ALB, and CB failure modes. Harris and Speicher's study [16] was utilized to define the prototype building and its applied loads (dead, live, and seismic). Lateral loads were resisted by the symmetrically located special moment frames along the East-West (E-W) direction and special concentrically braced frames along the North-South (N-S) direction in the prototype building. However, only the assessment of the moment frames will be presented in this study.

Figure 1 displays the plan and elevation view of the archetype building, with the location of tributary gravity loads allocated to the frames shaded. Span lengths are 9.1 meters (30 ft) and 6 meters (20 ft) in the E-W and N-S directions, respectively. The number of bays and bay widths affect the range of axial load ratios at the column ends. Analysis revealed that axial forces applied to the first-story columns ranged from 5% to 20%. Elkady and Lignos [7], Fogarty et al. [9], Wu et al. [11], and Ozkula et al. [12] demonstrated that the initial column axial force, which results from gravity loading, plays a crucial role in determining the cyclic responses of deep columns. Consequently, instead of using the shaded tributary area, 15% of the yield capacity of the column was generally applied as axial forces to the first-story columns.

The set of archetype buildings encompassed design variables addressing key issues related to the behavior of deep columns, such as the level of seismic design load, strong column weak beam (SCWB) ratio for boundary condition effects, and cyclic loading effects.

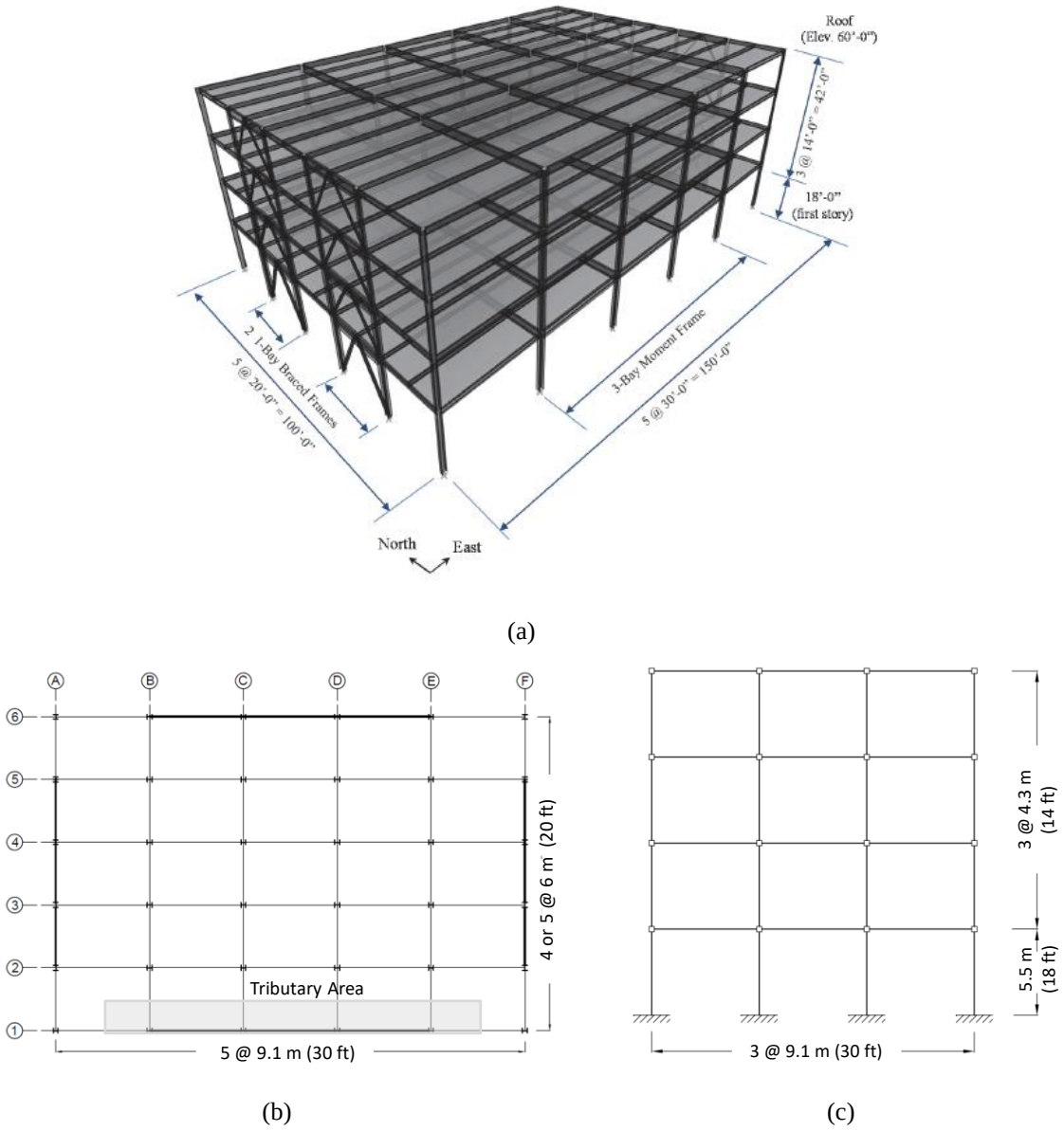

Figure 1 4-story Steel Moment Frame: (a) Isometric View of MC4 Prototype Building, (b) Plan View, (c) Elevation View

Table 1 presents the frame designations, with each frame named according to the failure mode criteria. The initial letters represent buckling modes, such as symmetric flange buckling (SFB), asymmetric flange buckling (ALB), and coupled buckling (CB). The second part of the designation provides information about the strong column weak beam ratio (SCWB), which is approximately 1 or 2. The final part of the designation offers details about the first column and beam bracing. All beams have slabs, so the top flange of the beams is braced, while the bottom flange is braced according to either AISC [17] requirements or the stiffening method proposed by Igawa and Ikarashi [24].

For example, the frame CB-SW1-CBTBS-IK has the following characteristics: CB represents coupled buckling; SW1 indicates an SCWB ratio of around 1; CBTBS denotes that the column (C) is braced at the bottom and top (BT) and the beam (B) has a slab (S); and IK signifies that stiffeners were used at the web of the beam based on the Igawa and Ikarashi method. In accordance with the failure mode classification presented by Ozkula et al. [13], Figure 2 illustrates the expected failure modes for the selected first-story column sections utilized in the study.

Finite Element Analysis of Arctype Building

Four-story moment frames were modelled with ABAQUS-CAE [15]. Four-node shell elements (SR4) were only used for the first story beams and columns while the remaining story elements were modelled with 2-node linear beam elements which adopts Timoshenko beam theory. However, since beam ends are the energy dissipation points, concentrated plasticity model suggested by Lignos and Krawinkler [5] utilized at these points.

Table 1 Frame Designation

Frame Designation	1st Story Members		Failure Mode	SCWB Ratio	Lateral Bracing	
	Column	Beam			Column	Beam
SFB-SW1-CBTBS	W14×370	W21×201	SFB	1	Bottom & Top	with Slab & AISC Bracing
SFB-SW1-CBTBS-IK					Bottom & Top	with Slab & Ikarashi Bracing
SFB-SW1-CTBS					Only Top	with Slab & AISC Bracing
SFB-SW1-CSBS					Through the length	with Slab & AISC Bracing
ALB-SW1-CBTBS	W24×131	W27×94	ALB	1	Bottom & Top	with Slab & AISC Bracing
ALB-SW1-CBTBS-IK					Bottom & Top	with Slab & Ikarashi Bracing
ALB-SW1-CTBS					Only Top	with Slab & AISC Bracing
ALB-SW1-CSBS					Through the length	with Slab & AISC Bracing
CB-SW1-CBTBS	W24×176	W27×114	CB	1	Bottom & Top	with Slab & AISC Bracing
CB-SW1-CBTBS-IK					Bottom & Top	with Slab & Ikarashi Bracing
CB-SW1-CTBS					Only Top	with Slab & AISC Bracing
CB-SW1-CSBS					Through the length	with Slab & AISC Bracing
SFB-SW2-CBTBS	W14×500	W21×201	SFB	2	Bottom & Top	with Slab & AISC Bracing
ALB-SW2-CBTBS	W30×173	W27×94	ALB	2	Bottom & Top	with Slab & AISC Bracing
CB-SW2-CBTBS	W30×261	W27×114	CB	2	Bottom & Top	with Slab & AISC Bracing

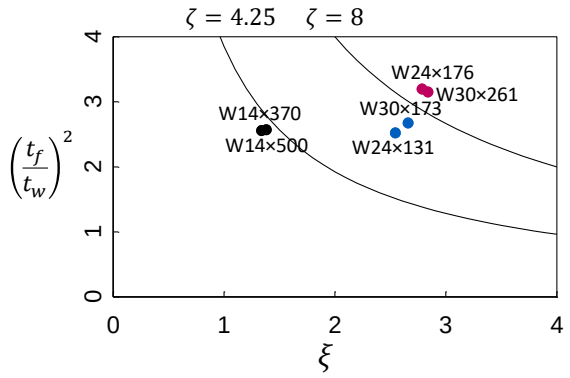

Figure 2 Buckling Modes of 1st Story Columns (Ozkula et al, 2023)

Column buckling only expected to occur at the column bases in moment frames therefore, it was crucial to model these columns with local buckling sensitive elements such as shells. However, since continuum finite element analysis are computationally expensive, by using the shell elements only at the first story columns, cut the computational effort significantly in this study.

First story RBS sections was modelled carrying out the cut of the beam flanges while at the upper floors, which beam elements were used to model columns and beams, an equivalent section with equal height but smaller width flange able to simulate the reduce section was introduced [see Figure 3(a)]. The width of the flange of equivalent

section was found starting from the definition of the plastic moment Z_{PL} as shown in Eqn. (1).

$$Z_{PL} = \frac{1}{4}\left[(A - t_w d)\left(d + d'\right) + (t_w d^2)\right] \qquad (1)$$

where t_w, d and A are the web thickness, the depth and the area of the section, and d' is the height of the web, respectively. Imposing Z_{PL} equal to the plastic modulus Z_{RBS} of the reduced section, Eqn. (1) can be solved in function of the area A and thus of the flange width b' of the equivalent section can be calculated.

Fix boundary conditions were applied at the frame columns while pin boundary conditions were used for leaning columns. Rigid body constraints capable to avoid possible local stress concentration and able to ensure that the relative positions of points remain constant throughout the analysis were used to tie the second floor's column top edges and the third floor's column bottom edges to a common reference point. Flexible supports with out-of-plane rotations and displacements restrained were used to prevent out of plane movement of the frame. Beam elements of the leaning columns are connected with hinges at each floor level [see Figure 3(b)].

The isotropic and kinematic hardening behaviors may both be simulated using a model from the ABAQUS-CAE material library. The hardening law, which contains both nonlinear isotropic and nonlinear kinematic hardening components, is based on the Von Misses yield surface, together with a related flow rule and its yield surface. This work made use of cyclical material features that had previously been examined by Ozkula et al. [12].

The initial geometric flaw is another element that affects the column capacity. By superimposing buckling modes generated from eigenvalue analysis, geometric flaws may be added to finite element models to cause local and global instabilities. According to AISC [17], L/1,000 is the recommended global out-of-straightness imperfection. ASTM [18] limits the local web and flange defects that are typical of the production process. Initial imperfections were also included in this study.

Results of Arctype Building and Discussion

The following issues were identified as the critical parameters for FE models to investigate the behavior of the first story columns in moment frames.

Cross Sectional Effect

Recent member-level test studies have revealed that cross-sectional differences influence column behavior and performance. The strong-axis dominance of slender sections renders them more susceptible to global buckling, such as lateral torsional buckling (LTB), while higher width-to-thickness ratios can increase the section's vulnerability to web or flange local buckling (LB). Within a specific limit of L/r_y, Ozkula et al. [13] proposed a parameter based on section slenderness properties to predict the governing buckling mode, which is utilized in this study.

Sections with high ductility and moderately low web and flange slenderness ratios often exhibit symmetric flange buckling (SFB) as the primary failure mechanism (commonly observed in shallow columns such as W12 and W14 columns). This method prevents out-of-plane, global-type member buckling by inducing in-plane plastic hinging at the column ends (or solely at the bottom end of first-story columns in a special moment frame (SMF) during practical implementation). These columns display remarkable consistency in their hysteresis response, even at higher drift levels. As section slenderness ratios increase, both flange and web local buckling modes emerge because the web is unable to provide sufficient rotational restriction to maintain fixed-ended boundary conditions for the half-width, unstiffened flange elements.

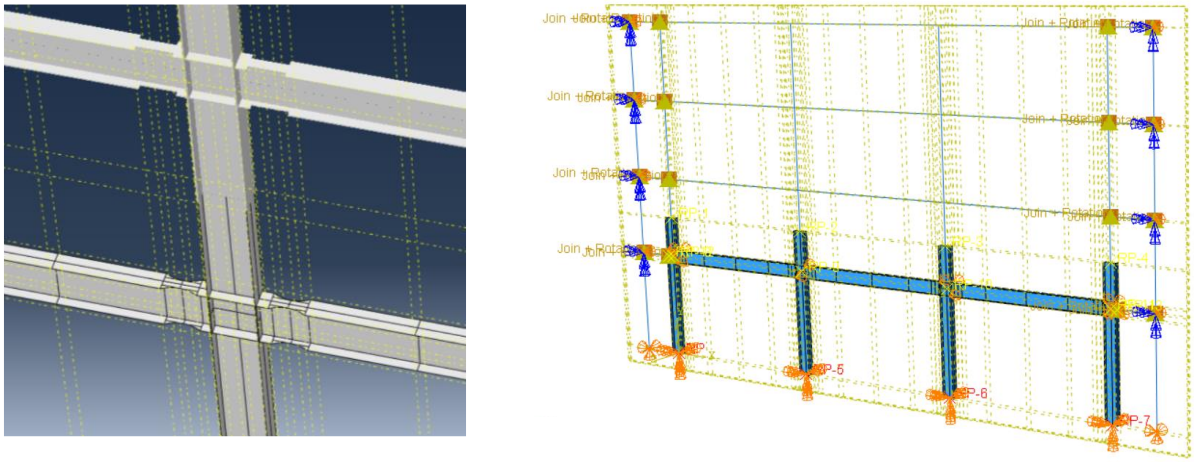

(a) (b)

Figure 3 Finite Element Model of Frames: (a) Details RBS section, shell and beam elements, (b) Boundary Conditions of Moment Frame

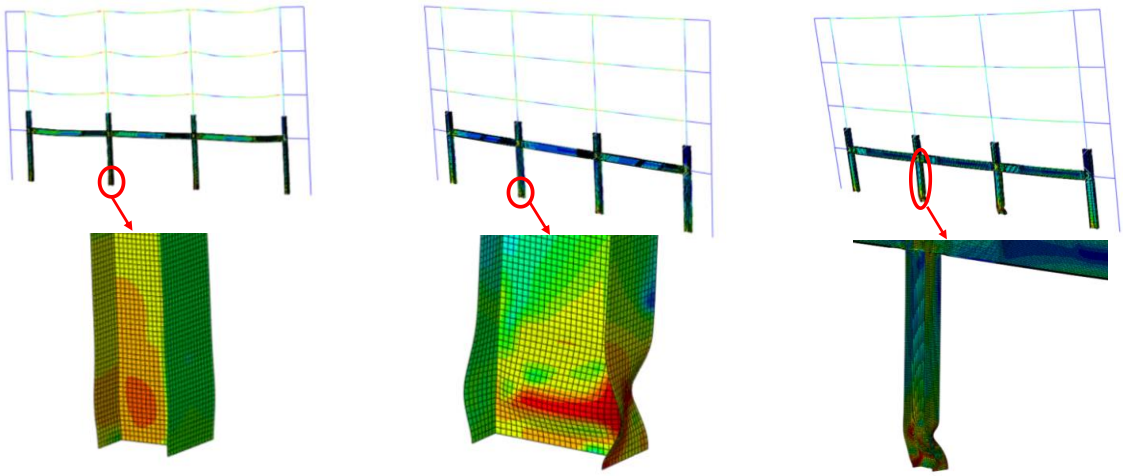

(a) (b) (c)

Figure 4 Effect of Cross Section: (a) SFB: W14×370, (b) ALB: W24×131, (c) CB: W24×176

The overall behavior of these sections proved to be more critical compared to symmetric flange buckling (SFB) type sections, as web and flange buckling led to a significant loss of strength when local buckling initiated. The coupled buckling (CB) mode is unique and encompasses several distinct characteristics. First, the column flanges were identified as stockier, with lower λ_f values, and highly ductile. Second, the yielding length—also known as the "plastic hinge" length—was substantial. The regions near the column ends continued to strain harden and achieve high flexural strength due to the delayed local buckling of these stockier sections, resulting in a considerably longer yielding zone at each end. Consequently, the column experienced lateral torsional buckling (LTB) due to the compressive flange's propensity to buckle along its strong axis. Third, the ductility (or capacity for inelastic deformation) was high.

Following Ozkula et al.'s [13] classifications, first-floor column sections were selected as shown in Table 1, and finite element modeling of these frames was performed to investigate the overall behavior and axial shortening of these sections. Figure 4 displays the failure modes of the selected first-story columns, which are consistent with the observations obtained from the experiments.

Effect of Axial Force Level

Columns in moment frames are subjected to combined axial and lateral loads. Axial loads consist of the loads at the governing tributary area and additional cyclic axial forces due to global overturning moments. Recent studies have determined that the cyclic behavior of deep columns exhibits significant strength degradation as a result of local buckling, and an increase in axial load level drastically exacerbates the post-buckling strength degradation and axial shortening of the column. To examine the effect of axial force level on the moment frame, three different axial load levels (C_a = 0.15, 0.30, 0.60) were selected. Consistent with component-level test results, frames with low axial load levels also performed better compared to their high axial force level counterparts, as demonstrated in Figure 5.

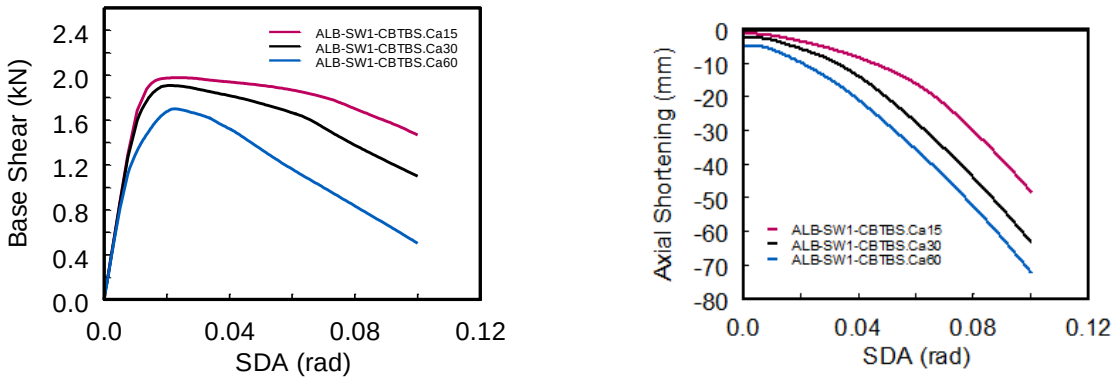

(a) (b)

Figure 5 Effect of Axial Force Level (ALB-SW1-CBTBS): (a) Base Shear vs. SDA, (b) Axial Short. (1st Story Inner)

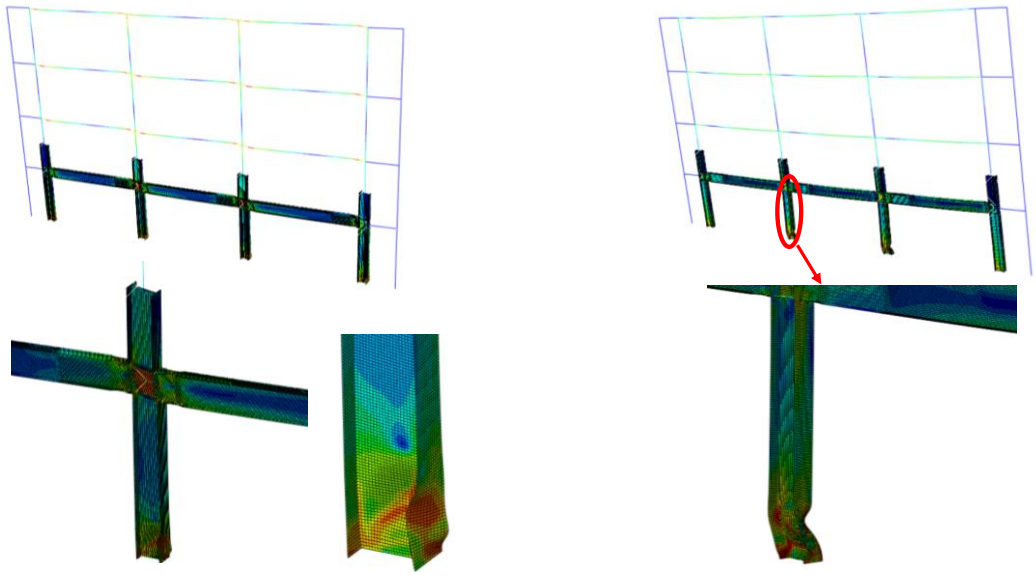

(a) (b)

Figure 6 Buckling Mode of Section W24×176 under Monotonic and Cyclic Loading: (a) Monotonic Loading, (b) Cyclic Loading

Effect of Monotonic vs. Cyclic Loading

The performance of moment-resisting frames can be significantly influenced by load and deformation history (Lignos and Krawinkler [5], Fogarty et al [9], Ozkula et al [12], FEMA 355C [19]). A comparison of monotonic and cyclic loading effects revealed that cyclic loading exposes specimens to a substantial amount of yielding and strain hardening, which results in global instabilities v(Ozkula et al, [12]). Due to the limited opportunity for significant yielding and strain hardening experienced by the column under monotonic loading, member-level column simulations indicated that out-of-plane global instability might not occur. Frame-level analyses were conducted, and the results of monotonic and cyclic loading corroborated the findings from member-level tests, as illustrated in Figure 6.

Effect of Strong Column Weak Beam Ratios

Due to inelastic deformations occurring in some stories, Scheider et al. [20] demonstrated that weak-column-strong-beam (WCSB) frames result in localized increases in seismic demands. To account for strain-hardening and mitigate the effects of concentrated plastic deformation, Nakashima and Sawaizumu [21] advised that column strength should exceed 120% of the beam's plastic moment capacity. Suita et al.'s [22] testing of a four-story moment frame on the E-Defense shaking table revealed increased beam strength due to strain hardening, slab effects, and material heterogeneity. The strong-column-weak-beam (SCWB) ratio was 1.5, and the columns were thin-walled tubes. However, a high slenderness ratio led to decreased column strength due to local buckling and reduced flexural strength. Lignos et al [5] proposed that using an SCWB ratio greater than 2 could prevent the first story collapse mechanism of this structure.

Current AISC seismic provisions aim to control column yielding by regulating the SCWB ratio, which balances the probable plastic capacity of the column. Recent research has shown that strain hardening during inelastic deformation, material variability, composite effects, variations in geometric corrections required for transferring beam moment capacities to the column, and fluctuations in inflection points' locations in beams and columns during seismic loading indicate that the current SCWB ratios do not prevent column yielding. Consequently, the SCWB ratio of the selected sections was revised and increased to 2, as shown in Table 1. With the SCWB ratio increased to 2, larger column sections had to be chosen, although beam sizes remained the same as those in frames with an SCWB ratio of 1. Figure 7 presents a comparison of SCWB ratios for various column depths. Figure 7(b) indicates that stiffness increases as the SCWB ratio rises for ALB-type columns, while this increase is limited for SFB-type and CB-type columns. Results also demonstrated that higher post-yield stiffness was obtained with lower SCWB ratio designs. This is primarily because column local buckling reduces significantly once the SCWB ratio increases; however, due to excessive buckling at the beam ends, the post-stiffness of the overall behavior decreases more.

Effect of Beam Bracing

AISC Seismic Provisions [14] require that the lateral support for beams should be applied at all plastic hinge locations, and that additional bracing needs to be applied at regular intervals (L_b) from these locations.

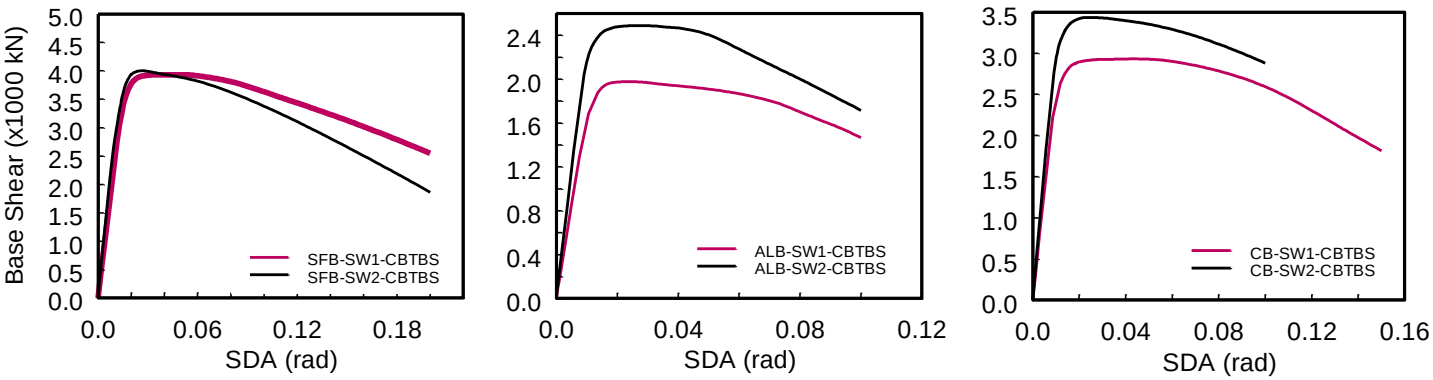

(a) (b) (c)

Figure 7 Effect of SCWB Ratio under Monotonic Loading: (a) SFB-SW1-CBTBS vs. SFB-SW2-CBTBS, (b) ALB-SW1-CBTBS vs. ALB-SW2-CBTBS, (c) CB-SW1-CBTBS vs. CB-SW2-CBTBS

Figure 8 Beam Bracing Samples

Trahair [23] provides an extensive overview of studies on the stability of lateral torsional buckling (LTB). Practice has led to the derivation of the form for elastic LTB for continuous bending of a doubly symmetric broad flange section under pure bending, which is a function of warping constant, C_w, torsional constant, J, the moment of inertia about the weak axis, I_y, LTB modification factor C_b .

AISC Seismic Provision requires use of stability bracing to restrain the LTB of structural steel or concrete-encased beams subjected to flexure. Beam bracing shall have a maximum spacing as shown in Eqn.(2).

$$L_b = 0.19 r_y E/\left(R_y F_y\right) \quad (2)$$

AISC 341 suggests using these bracing members near concentrated forces, changes in cross section, and other locations where analysis indicates that the plastic hinge will likely occur.

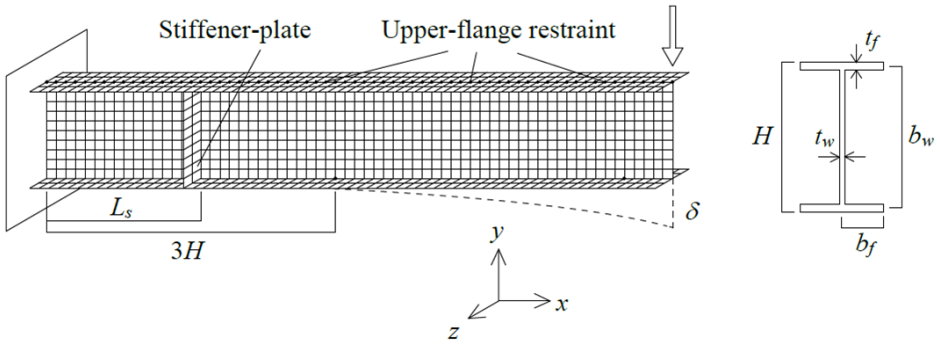

Figure 9 Analytical Model [Igawa and Ikarashi (2020)]

However, there is no requirement on the strength and capacity of the stability braces which are utilized in moment frames. Figure 8 shows some stability samples widely used in US.

Transition and rotation of the upper flange of the beam cross section is continuously and intermittently restrained by the floor slab which restraint acts effectively against the out-of-plane lateral buckling. Igawa and Ikarashi [24] proposed that using stiffener-plates is one of the effective methods of stiffening against the buckling of members rather than adding external bracing members.

Figure 9 shows the analytical model used by Igawa and Ikarashi [24] to define the location of the stiffener plate from fix-end to the stiffener plate. Igawa and Ikarashi [24] utilize an equation to predict if the buckling mode of the beam will be local or global buckling. In this study, Igawa and Ikarashi [24]'s approach is compared with the AISC defined stability bracing requirement [see Eqn.(2)] to be able to eliminate the stability braces which was shown in Figure 8.

Table 2 tabulated the expected failure modes and stiffener locations of the beams. Figure 10 and Figure 11 shows the buckling modes of beam elements (zero axial force) with section W27×114 and W21×147 which expect to have CB and ALB failure modes, respectively. Both Ozkula et al. [13] and, Igawa and Ikarashi [24] predicts the same failure modes with different approaches. Figure 10 shows the buckling modes under different bracing conditions. If the same section braced at the top flange but remains unbraced at the bottom flange [Figure 10 (b)], CB still observed however as show in Figure 12 strength degradation of this section is much more compare to the section braced at the top and bottom flanges. Once the section braced at the top and bottom flange or stiffened at the certain location defined by Igawa and Ikarashi [24], the strength degradation reduces since the local bucking delayed (see Figure 12). Figure 11(a) shows that if the unbraced length of the section is too long (30 ft), LTB mode governs. However, once the global slenderness ratio is less than 120, same section buckles in ALB mode. Unlike CB type section (W27×114), behavior of ALB type beam member (W21×147) did not affected by the bracing as shown in Figure 12.

Table 2 Beam Failure Modes and Stiffener Locations from the Beam-to-Column Joint

Frame Name	Beam Section	$\frac{WF}{\lambda_b}$	L_{se}	Ikarashi Buckling Prediction	Ozkula Buckling Prediction
SFB-SW1-CBTBS	W27X114	1.290753	101.8552	LB	CB
	W27X102	1.367448	103.4535	LB	CB
ALB-SW1-CBTBS	W27X94	1.462859	18.68677	PLB	ALB
	W27X84	1.614272	17.8222	PLB	ALB
CB-SW1-CBTBS	W21X201	1.314322	99.86283	LB	CB
	W21X147	1.639897	20.26742	PLB	ALB

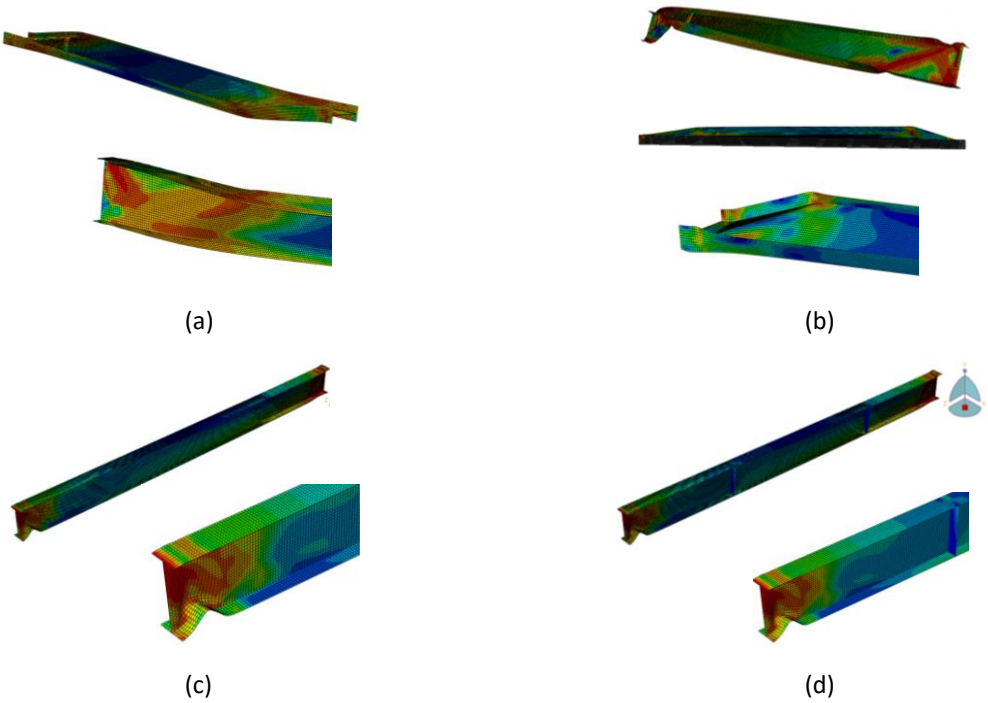

Figure 10 Bracing Conditions of Section W27×114: (a) Top & Bottom Flange Unbraced, (b) Bottom Flange Unbraced, (c) AISC Bracing, (d) Stiffener at the Web

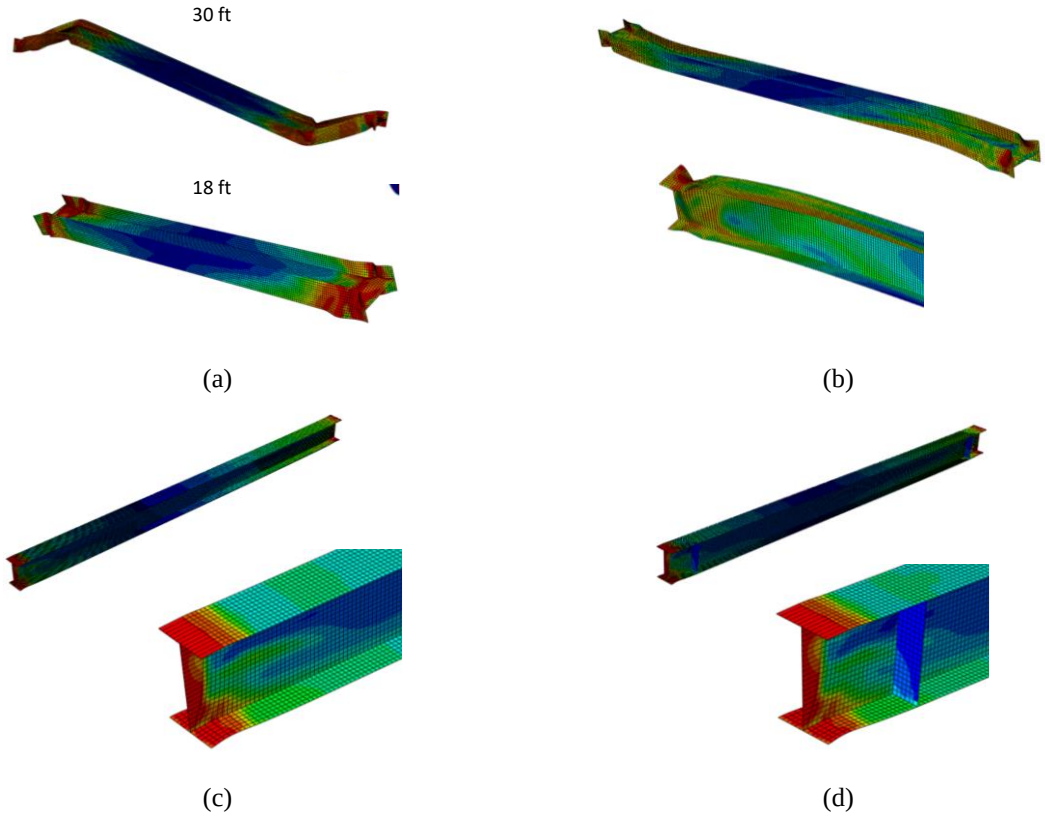

Figure 11 Bracing Conditions of Section W21×147: (a) Top & Bottom Flange Unbraced, (b) Bottom Flange Unbraced, (c) AISC Bracing, (d) Stiffener at the Web

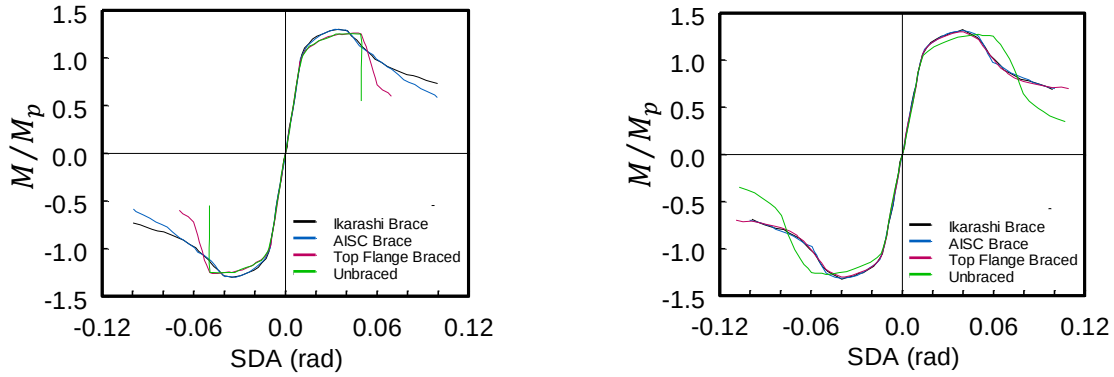

(a) (b)

Figure 12 Brace Effect on Beam's Post Buckling Strength and Stiffness: (a) Section W27×114, (b) Section W21×147

Figure 13 illustrates that the application of stiffeners to beam sections is only effective when ALB-type columns are utilized. As SFB-type sections do not experience extensive local buckling and CB-type sections are subject to global buckling, beam bracing does not contribute to enhancing the post-strength of the frame.

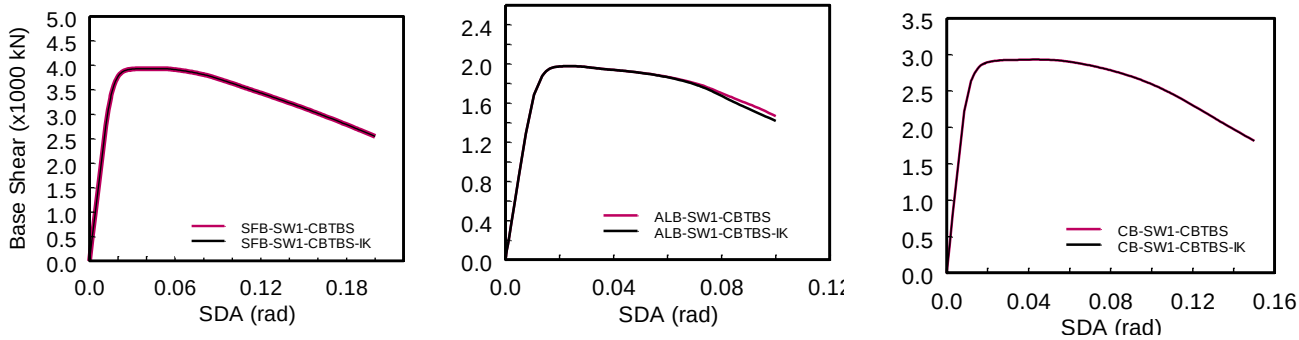

(a) (b) (c)

Figure 13 Effect of Beam Bracing under Monotonic Loading: Base Shear vs. SDA: (a) SFB-SW1-CBTBS vs. CBTBS-IK, (b) ALB-SW1-CBTBS vs. CBTBS-IK, (c) CB-SW1-CBTBS vs. CBTBS-IK

(a) (b)

Figure 14 Column Bracing Samples: (a) Bracing at the Top Flange, (b) Bracing at the Top and Bottom Flange

Effect of Column Bracing

Warping constant, C_w is depend upon the square of the distance between the centroid of the flanges, deeper wide flange sections generally have higher torsional resistance, however this occurs through increased resistance to warping torsion rather than St. Venant torsion. Slender column sections may experience higher normal stresses due to warping restraint, and therefore earlier yielding of flanges. The warping component of LTB is more severely reduced by a longer unsupported length, L_b. As a result, LTB capacity of deep columns is expected to be much more depend on the lateral support than shallow columns, which are dominated by St. Venant torsion. Even though, AISC specifies the maximum length of stability braces for beam

elements, there is no requirement for column bracing throughout the length. However, AISC Seismic Provisions [14] suggests that when the webs of the beams and column are coplanar, and column is shown to remain elastic outside of the panel zone, column flanges at beam-to-column connections shall require stability bracing only at the level of the top flanges of the beams [see Figure 14(a)]. When a column cannot be shown to remain elastic outside of the panel zone, it can be braced at the levels of both top and bottom beam flanges as shown in Figure 14(b). Figure 15 shows that bracing column at the top and bottom flange level slightly improves the overall behavior for ALB and CB-type columns however it is not effective for SFB-type columns. Quasi static loading case also shows similar trend as shown in Figure 16. Column bracing at the top and bottom of the column also helped reducing the axial shortening of the column as shown in Figure 17.

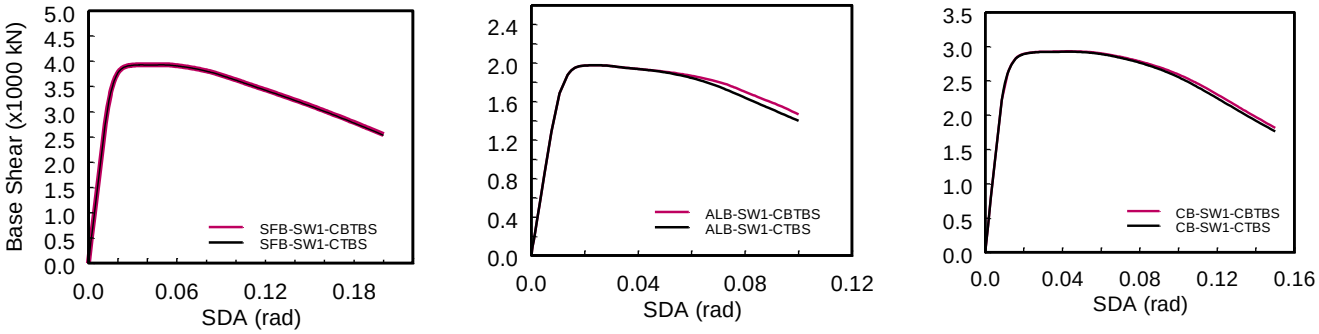

(a) (b) (c)

Figure 15 Effect of Column Bracing under Monotonic Loading: (a) SFB-SW1-CBTBS vs. CTBS, (b) ALB-SW1-CBTBS vs. CTBS, (c) CB-SW1-CBTBS vs. CTBS

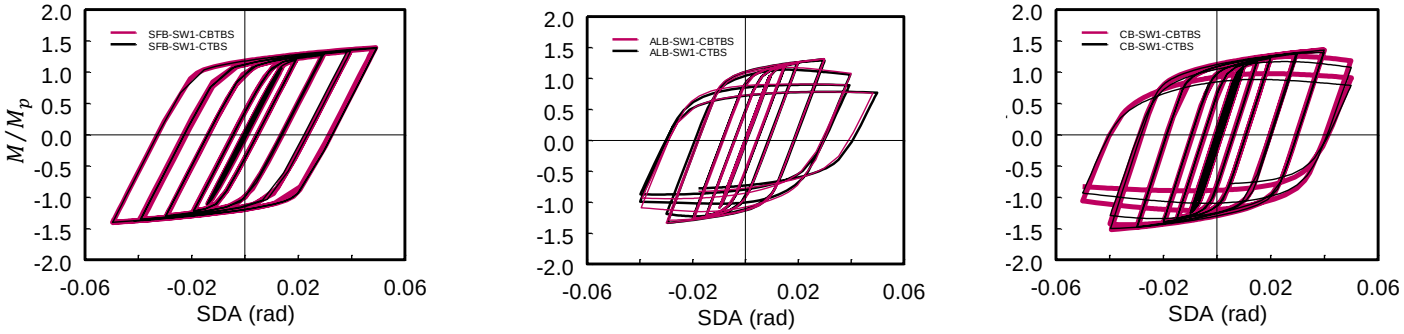

(a) (b) (c)

Figure 16 Effect of Column Bracing under Cyclic Loading: (a) SFB-SW1-CBTBS vs. CTBS, (b) ALB-SW1-CBTBS vs. CTBS, (c) CB-SW1-CBTBS vs. CTBS

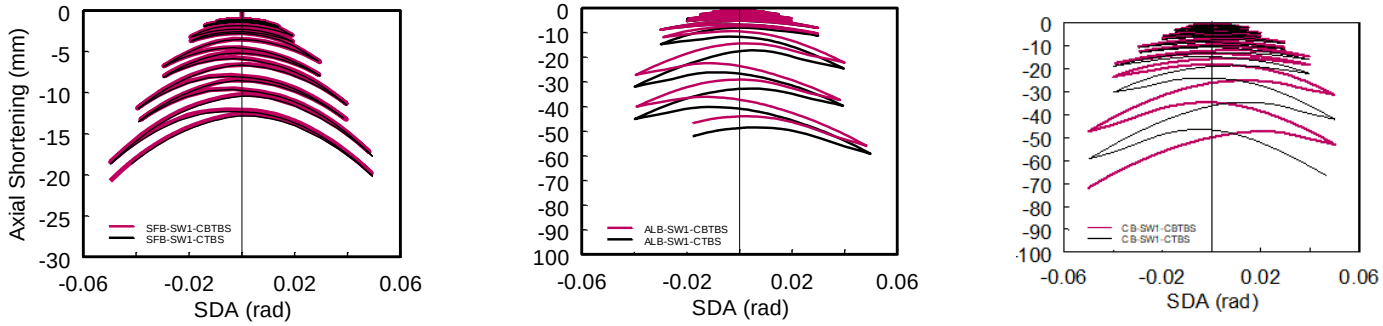

(a) (b) (c)

Figure 17 Effect of Column Bracing under Cyclic Loading: (a) SFB-SW1-CBTBS vs. CTBS, (b) ALB-SW1-CBTBS vs. CTBS, (c) CB-SW1-CBTBS vs. CTBS

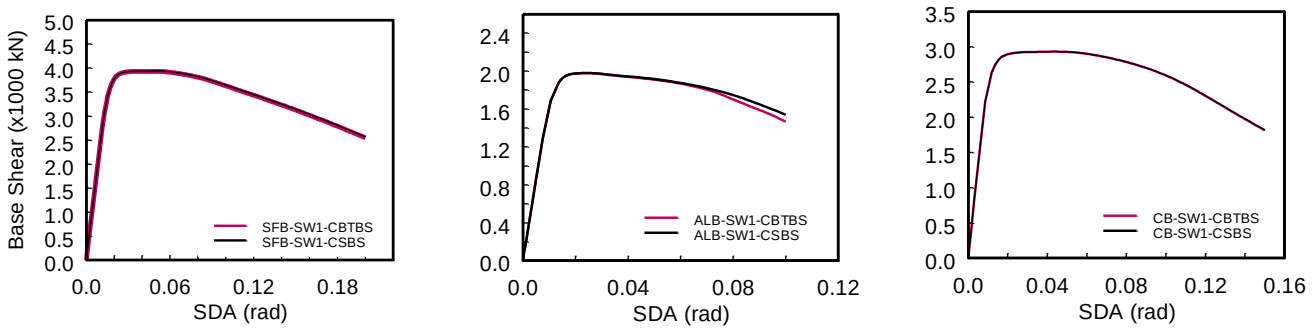

(a) (b) (c)

Figure 18 Effect of Column Bracing with Stiffeners under Monotonic Loading: (a) SFB-SW1-CBTBS vs. CSBS, (b) ALB-SW1-CBTBS vs. CSBS, (c) CB-SW1-CBTBS vs. CSBS

Effect of Column Bracing with Stiffeners

The impact of beam bracing through the addition of stiffeners has been previously discussed. Although the equations proposed by Igawa and Ikarashi [24] were based on analytical and experimental test results for beam sections, their approach was also applied to column stiffening in this study. Figure 18 reveals that, similar to beam bracing conditions, column bracing only enhances the performance of ALB-type sections. However, the elimination of braces contributes to a reduction in construction costs and frees up space in the beam-to-column connection regions (see Figure 14). Further research could be conducted to account for the effect of axial force in the equation.

Summary and Conclusions

The comprehensive seismic design of frames in this study has been carried out by adhering to the US design codes, specifically the ASCE 7-16 [25] and the AISC Seismic Provisions [14]. These design codes provide detailed guidelines and requirements for designing structures to withstand seismic forces to ensure their safety and stability during earthquake events. In this context, the AISC quasi-static loading is considered for the design and analysis of the frames. Quasi-static loading refers to the slow application of loads on a structure, which simulates the effects of seismic forces without the need for a full dynamic analysis. This method is particularly useful in assessing the performance of the structural system, including its strength and stiffness, under various load conditions that mimic the impact of earthquakes. The ASCE 7-16 [25] code defines the procedures for calculating seismic loads, such as the seismic base shear and story forces, which are used in the design and analysis of the structural system. The code also establishes the criteria for selecting appropriate seismic design categories, response modification factors, and system overstrength factors, which are essential in determining the structural system's seismic performance requirements.

To evaluate the behavior of deep columns compared to their shallow counterparts, multiple ABAQUS analyses were performed. A total of fifteen four-story steel SMFs were investigated, focusing on four key factors: 1) Column bracing; 2) Beam bracing; 3) Column stiffening; and 4) Strong Column Weak Beam (SCWB) ratio. Three governing buckling modes defined by Ozkula et al. [12] were utilized in this study: symmetric flange buckling (SFB), anti-symmetric local buckling (ALB), and coupled buckling (CB) to categorize the moment frames (see Table 1 for frame designations).

From the numerical simulation results, the following conclusions can be drawn:

- Previous member-level test results demonstrated that the ratio of local slenderness ratios (λ_f/λ_w) for local buckling had a significant effect on the buckling mode (local versus global buckling), as long as the member slenderness (λ_L) is less than 120, as proposed by Ozkula et al. [12]. Frame analyses also confirmed the importance of these parameters.
- Analyses showed that the level of axial force significantly influences the plastic rotation capacity and post-buckling stiffness. The presence of axial compression produced significant local buckling and axial shortening, which created additional stresses on adjacent beams.
- Since the column did not have the chance to undergo considerable yielding and strain hardening as its cyclic counterpart did, member-level column simulations revealed that out-of-plane global instability might not occur under monotonic loading. The results of the member-level tests were validated by the frame-level analysis, as well as by the results of monotonic and cyclic loading.
- Comparing -CBTBS versus -CTBS frames showed that additional lateral bracing at the level of the top flange of the beam moderately improved the capacity of the frame for ALB-type columns, slightly for CB-type columns, and did not affect the behavior for SFB-type columns.
- Comparing -SW1-CBTBS and -SW2-CBTBS suggests that stiffness increases as the SCWB ratio increases for ALB-type columns, while this increase is limited for SFB-type and CB-type columns. Results

also showed that higher post-yield stiffness was obtained with lower SCWB ratio design. This is mainly because the column local buckling reduces significantly once the SCWB ratio increases; however, due to excessive buckling at the beam ends, the post stiffness of the overall behavior decreases more.

- Igawa and Ikarashi [24]'s approach was compared with the AISC-defined stability bracing requirement to potentially eliminate stability braces. Analysis results showed that adding stiffeners to the beams slightly improved the overall capacity of the frame but did not change the failure mode of the columns.
- Even though AISC specifies the maximum length of stability braces for beam elements, there is no requirement for column bracing throughout the length. However, AISC Seismic Provisions suggest that when the webs of the beams and column are coplanar, and the column is shown to remain elastic outside of the panel zone, column flanges at beam-to-column connections shall require stability bracing only at the level of the top flanges of the beams. Therefore, two frames (-CBTBS and -CTBS) were compared to investigate the behavior of column bracing at the top and bottom flanges. Results showed that additional lateral bracing at the level of beam bottom flanges for beam-to-column connections slightly improved the capacity of the frames with ALB and CB-type columns, while it did not affect the capacity for SFB-type columns. Therefore, it is suggested to brace columns at both the top and bottom of the beam flanges, except for the SFB-type sections.
- Although the equations proposed by Igawa and Ikarashi [24] were based on the analytical and experimental test results of beam sections, their approach was also utilized for column stiffening in this research. Results demonstrated that adding stiffeners to the column slightly improved the capacity of the ALB-type columns only.

In conclusion, this study provided valuable insights into the behavior of steel special moment frames, considering various factors such as column and beam bracing, column stiffening, and SCWB ratios. The results can guide future research and potential improvements to the AISC Seismic Provisions, with the aim of enhancing the performance of steel structures in seismic events.

Ethics committee approval and conflict of interest statement

There is no conflict of interest with any person / institution in the article prepared.

Authors' Contributions

All study conducted by the author of this paper.

Acknowledgement

This study was supported by the Scientific and Technology Research Council of Turkey (TUBITAK) through fellowship program.

References

[1] FEMA. "Prestandart and commentary for the seismic rehabilitation of buildings", FEMA 356, *Federal Emergency Management Agency*, Washington D.C., 2000.

[2] Ibarra L, Medina R, Krawinkler H."Collapse assessment of deteriorating SDOF systems". Proceedings of the 12th European conference on earthquake engineering, Elsevier Science Ltd, London, September 2002.

[3] Ibarra, L.F., Medina, R.A., and Krawinkler H. "Hysteretic models that incorporate strength and stiffness deterioration," *Earthquake Engineering and Structural Dynamics*, 34:1489-1511, 2005.

[4] Rahnama, M., Krawinkler, H. "Effects of Soft Soil and Hysteresis Model on Seismic Demands", *John A. Blume Earthquake Engineering Center*, 1993.

[5] Lignos, D.G., Krawinkler, H. "Deterioration modeling of steel components in support of collapse prediction of steel moment frames under earthquake loading." *Journal of Structural Engineering*, 137(11), 1291-1302, 2011.

[6] Newell, J.D. and Uang, C.-M. "Cyclic behavior of steel wide-flange columns subjected to large drift," *Journal of Structural Engineering*, Vol. 134, No. 8, 1334-1342, ASCE, 2008.

[7] Elkady, A., and Lignos, D.. "Dynamic stability of deep slender columns as part of special MRFs designed in seismic regions: finite element modeling." *Proc., 1st Inernational Conference on Performance-Based and Life-Cycle Structural Engineering (PLSE)*, Hong Kong, China, 2012.

[8] Cheng, X., Chen, Y., and Nethercot, D.A. "Experimental study on H-shaped steel beam-columns with large width-thickness ratios under cyclic bending about weak-axis." Engineering Structures, 49, 264-274, 2013.

[9] Fogarty, J., and El-Tawil, S. "Collapse resistance of steel columns under combined axial and lateral loading", *Journal of Structural Engineering*, Vol. 142, No. 1, ASCE, 2016.

[10] Suzuki, Y., and Lignos, D.G. "Large scale collapse experiments of wide flange steel beam-columns." *8th International Conference on Behavior of Steel Structures in Seismic Areas*, Shanghai, China, 2015.

[11] Wu, T.U., El-Tawil, S., and McCormick, J. "Highly ductile limits for deep steel columns," *J. Struct. Eng.* 144 (4): 04018016, 2018.

[12] Ozkula, G., Harris, J., and Uang, C.-M. "Observations from cyclic tests on deep, wide-flange beam-columns", *Engineering Journal*, 1st Quarter, AISC, 45-59, 2017.

[13] Ozkula, G., Harris, J., and Uang, C.-M. "Classifying cyclic buckling modes of steel wide-flange columns under cyclic loading," *Structures Congress*, 155-167, ASCE/SEI, Denver, Colorado, 2017.

[14] AISC. *Seismic provisions for structural steel buildings*, ANSI/AISC 341-05, American Institute of Steel Construction Chicago, IL, 2015.

[15] ABAQUS-FEA/CAE. Dassault Systemes Simulia Corp., RI, 2011.

[16] Harris J.L, Speicher, M.S. "Assessment of first generation performance-based seismic design methods for new buildings, Volume 1: Special moment frames", *National Institute of Standards and Technology*, Feb. 2015.

[17] AISC. *Specification for structural steel buildings*, ANSI/AISC 360-05, American Institute of Steel Construction, Chicago, IL, 2015.

[18] ASTM. *Standard definitions of terms relating to constant- amplitude low-cycle fatigue testing*, ASTM Standard E466, 2003.

[19] FEMA. "State of the art report on system performance of steel moment frames subject to earthquake ground shaking", FEMA 355C, *Federal Emergency Management Agency*, Washington D.C, 2000.

[20] Schneider, S.P., Roeder, C.W., Carpenter, J.E., "Seismic behavior of moment-resisting steel frames: experimental study", *Journal of Structural Engineering*, 119(6), 1885-1902, 1993.

[21] Nakashima, M., Sawaizumi S., "Column-to-beam strength ratio required for ensuring beam-collapse mechanisms in earthquake responses of steel moment frames", Proceeding of the 12th World Conference, 2000.

[22] Suita, K., Yamada, S., Tada, M., Kasai, K., Matsuoka, Y., and Sato, E. "Results of recent e-defense tests on full-scale steel buildings: Part 1 − Collapse experiment on 4-story moment frame," *Proceedings* Structures Congress, Vancouver, Canada, 2008.

[23] Trahair, N.S., "Flexural-Torsional Buckling of Structures", *Taylor and Francis*, 1993.

[24] Igawa, N. and Ikarashi, K. "Effect of stiffener position on buckling behavior of H-shaped steel beam with upper flange restraint", *Thesis*, Department of Architecture and Building Engineering, Tokyo Institute of Technology, Japan, 2020.

[25] ASCE. "Minimum design loads for buildings and other structures", ASCE 7, *American Society of Civil Engineers*, Reston, VA, 2016.